

**Proceedings of the Korean Nuclear Society Spring Meeting**

Cheju, Korea, May 2001

**Evaluation of Neutron Induced Cross Sections on  $^{109}\text{Ag}$**

Y. D. Lee and J. H. Chang

Korea Atomic Energy Research Institute  
P.O. Box105, Yusung, Taejon, Korea 305-600

**Abstract**

The neutron induced cross sections for  $^{109}\text{Ag}$  were evaluated from 1 keV to 20 MeV. The parameters of optical model potential depending on incident neutron energy were extracted based on the experimental data and the s-wave strength function was calculated. The reaction cross sections produced by GNASH and EMPIRE were analyzed. The model calculated cross sections were compared with the experimental data and other evaluated files (ENDF/B-VI, JENDL3.2 and JEF-2.2) on the total, elastic and reaction cross sections. The model calculated total and capture cross sections gave good agreement with the reference experimental data. The evaluated cross sections were compiled to ENDF-6 format.

**1. Introduction**

Neutron cross sections of fission product nuclides are important to predict burnup performance of fission reactors. Enhanced neutron cross sections will play an important role in several applications, including criticality calculation in spent nuclear fuel storage design and reactor core design. Additionally, reaction cross sections of fission products are needed for activation analysis and radiation damage estimation of structural materials in a reactor.

Generally, the neutrons released by fission in a light water reactor core have a mean energy of 1-2 MeV in their energy spectrum. These neutrons lose their energy continuously by interacting with fuel materials, structure materials and moderator in a reactor. Many fission products have large neutron capture cross section at the

intermediate and thermal neutron energy. The absorbed neutrons by fission products have a large portion in the total loss of neutrons.

As one of the prior fission products influencing reactivity greatly in a fission reactor, cross sections of  $^{109}\text{Ag}$  were evaluated from the unresolved resonance energy region up to 20 MeV.  $^{109}\text{Ag}$  is stable nucleus and mainly accumulated by beta decay from  $^{109}\text{Pd}$  and by electron capture from  $^{109}\text{Cd}$ . It is produced by direct fission from  $^{235}\text{U}$  and  $^{239}\text{Pu}$  fissile materials in a reactor as well.  $^{109}\text{Ag}$  is a significant fission product nuclide in fission reactor concerning neutron absorption loss. Accurate neutron capture cross section in the keV energy range is important in a reactor.

The cross sections were generated by nuclear model calculation and the evaluation was based on the reference experimental data. For theoretical neutron cross sections, spherical optical model, statistical model and pre-equilibrium model were applied to generate the total, elastic scattering and reaction cross sections. The optical model potential depending on the incident neutron energy was searched using a graphical interface to the ABAREX[1]. Parameters were selected by comparing the model calculated values with experimental total[2] and elastic cross sections. The produced s-wave strength function by ABAREX from the searched optical model potential parameters was compared with that of the evaluated in the resonance region[3].

Nuclear reaction cross sections were calculated by GNASH[4], exciton model code, and EMPIRE-II[5], quantum mechanical approach using multistep direct(MSD) and multistep compound(MSC), in pre-equilibrium energy range. GNASH calculation did not involve the width fluctuation correction. However, the evaluation using EMPIRE-II involves the width fluctuation correction and the dynamic approach to level densities (including energy dependent in level density parameter). EMPIRE-II offers the ENSDF nuclear level library. The cross sections evaluated are (n, tot), (n, n), (n, n'), (n,  $\gamma$ ), (n, p), (n,  $\alpha$ ), (n, 2n), (n, 3n), (n, n $\alpha$ ) and (n, np). The calculated cross sections are graphically compared with the experimental data and evaluated files (ENDF/B-VI, JENDL-3.2 and JEF-2.2). The evaluated results are compiled to ENDF-6 format and will improve ENDF/B-VI.

## 2. Optical Model Potential

The optical model was used to provide the theoretical total and scattering cross sections by spherical nuclei of neutrons with energies up to 20 MeV, above resolved resonance region. To obtain proper potential parameters, the Woods-Saxon well is used for the real optical model potential

$$V(r) = -V / \{1 + \exp((r - R_v)/a_v)\} \quad (1)$$

where  $V$ ,  $a_v$  are the potential strength and diffuseness of the potential respectively and the nuclear radius  $R_v$ , related to mass number  $A$ , is given by

$$R_v = r_v A^{1/3} \quad (2)$$

The derivative Woods-Saxon shape is used for the imaginary part of the optical model potential.

$$W(r) = -4W \exp((r - R_w)/a_w) / \{1 + \exp((r - R_w)/a_w)\}^2 \quad (3)$$

where  $W$ ,  $R_w$ ,  $a_w$  are potential strength, radius, diffuseness. Generally, Thomas form is taken in the optical model potential for spin-orbit coupling

$$V_{s-o}(r) = (2 \bar{L} \cdot \bar{S}) V_{so}(2/r) \{d/dr(1/[1 + \exp((r - R_{so})/a_{so})])\} \quad (4)$$

where  $\bar{L} \cdot \bar{S}$  is the dot product of the orbital and spin angular momentum operator. The spin-orbit coupling does not give much influence on neutron reaction cross sections.

The spherical optical model potential depth and radius of real and imaginary part were defined as a function of incident neutron energy.

$$V = V_o + V_1 \times E_n \quad , \quad r_v = r_o + r_1 \times E_n \quad (5a)$$

$$W = W_o + W_1 \times E_n \quad , \quad r_w = r_{wo} + r_{w1} \times E_n \quad (5b)$$

$E_n$  is an incident neutron energy. The 13 potential parameters ( $V_o$ ,  $V_1$ ,  $r_o$ ,  $r_1$ ,  $a_v$ ,  $W_o$ ,  $W_1$ ,  $r_{wo}$ ,  $r_{w1}$ ,  $a_w$ ,  $V_{so}$ ,  $r_{so}$ ,  $a_{so}$ ), including spin orbit interaction, were searched simultaneously and the result was summarized in Table I. These searched parameters calculate s-wave strength function( $S_o$ ) at 1keV incident neutron energy. Table II shows  $S_o$  calculated from the selected potential parameters and evaluated from the recent measurement.  $S_o$  will gives help to get the closer total cross section to experimental data and match the total by resonance parameters at unresolved region. For proton, deuteron, triton, alpha particle decay, Perey, Lohr-Haeberli, Becchetti-Greenless, Moyer potential parameters [5] were used respectively.

### 3. Calculation

As a preliminary step, retrieve and analyze the available experimental data and the evaluated files (ENDF/B-VI, JENDL-3.2 and JEF-2.2). GNASH, including Hauser-Feshbach theory to calculate complicated sequences of reaction and pre-equilibrium correction, was used to calculate the reaction cross sections. However, there is restriction in GNASH to describe the angular distribution. EMPIRE-II code uses Hauser-Feshbach decay for particles and gamma rays with the width fluctuation corrections. The multi-step direct model in EMPIRE-II takes care of the inelastic

scattering to vibrational collective levels and decay information.

There was total cross section calculation from the searched optical model potential. Fig. 1 shows the comparison of the calculated total cross section to experiment data and other evaluated files. Fig. 1 shows somewhat difference at low energy range between the current evaluation and ENDF/B-VI. However, the theoretical model calculation gave good agreement with the experimental data in the measured energy range and there was no much difference from other evaluated results. Fig. 2 shows the elastic scattering cross section. The calculated elastic scattering cross section follows the other evaluated files above first excited energy.

Fig. 3 is the comparison of capture cross section by GNASH and EMPIRE-II with experimental data[6,7,8,9,10,11] and other evaluated results. The calculated results by GNASH and EMPIRE-II follow the experimental data well. However, above 20 keV, no experimental data exist, the difference is shown between the evaluations in the figure. Fig. 4 shows the capture cross section in the limited measured data range. The calculated by EMPIRE-II follows the measurements[6,7] well. Fig. 5 shows the inelastic scattering cross section. GNASH has unusual prominent peak at low energy. On the other hand, EMPIRE-II shows the reasonable graph shape like other evaluation files. Moreover, EMPIRE-II gave good agreement with experimental data[12,13,14], even in meta-stable inelastic scattering cross section. Specially, above 12 MeV, EMPIRE-II has the higher cross section value than that by GNASH, mainly contributed by multistep direct reaction.

Fig. 6 is the  $(n, p)$  cross section from the evaluations and experimental data[15,16,17,18,19,20,21,22]. EMPIRE-II shows the sudden drop after 15 MeV energy. Fig. 7 shows the  $(n, \alpha)$  cross section. Figs. 8, 9 and 10 represent the  $(n, 2n)$ ,  $(n, n\alpha)$  and  $(n, np)$  cross sections respectively. Unfortunately, there are no experimental data for those reactions. The present evaluation complements the evaluation below the fast neutron energy region.

#### **4. Discussion of Results**

ABAREX was effective to get the proper optical model potential depending on the incident neutron energy. The selected optical model potential parameters represent the theoretical calculation of cross sections properly in the measured energy range and the parameters are expanded in the whole evaluation energy range. The *s*-wave strength function was also helpful to generate the total cross sections closer to experimental data.

The calculated capture cross sections by GNASH and EMPIRE-II were in good

agreement with the measured data. However, GNASH had unusual shape in inelastic scattering cross section. On the other hand, EMPIRE-II including width fluctuation correction was successful to produce the inelastic scattering cross sections, even for the meta-stable. Evaluated cross sections by EMPIRE-II were quite well agreed with the available experimental data. Therefore, EMPIRE-II is preferable in reaction cross section generation up to 20 MeV.

### Acknowledgements

This work is performed under the auspice of Korea Ministry of Science and Technology as a long-term R&D project.

### References

- [1] D. Lawson, ``ABAREX\_A Neutron Spherical Optical-Statistical Model Code,`` in Workshop on Computation and Analysis of Nuclear Data Relevant to Nuclear Energy and Safety, pp447-516, Trieste, Feb. 10 – Mar. 13, 1992.
- [2] Ju.V. Dukarevich, A.N. Djumin and D.M. Kaminker, ``Total Neutron Cross Sections of Isotopes and the Isobaric Spin Term of Nuclear Potential.,`` J. NP/A, 92,(2), 433, 1967.
- [3] S-O. Oh, J. H. Chang and S. Mughabghab, Neutron Cross Section Evaluations of Fission Products below the Fast Energy Region, Report BNL-NCS-67469, 2000.
- [4] P. G. Young and E. D. Arthur, GNASH: A Preequilibrium, Statistical Nuclear-Model Code for Calculation of Cross Section and Emission Spectra, Oak Ridge National Laboratory, RSIC Code Package PSR-125.
- [5] M. Herman, Empire-2: Statistical Model Code for Nuclear Reaction Calculations IAEA, Vienna, 2000.
- [6] M.V. Bokhovko, L.E. Kazakov, V.N. Kononov and E.D. Poletaev, ``Neutron Radiative Capture Measurements in Simver in the Energy Range 4-400 keV,`` J,YK,,(2),21,1987.
- [7] R.L.Macklin, ``Neutron Capture Cross Sections of the Silver Isotopes 107-Ag and 109-AG from 2.6 to 2000 keV,`` J, NSE, 82, 400, 1982.
- [8] M. Mizumoto ``Neutron Radiative Capture and Measurements of Ag-107 and Ag-109. J, NST, 20, (11), 883, 1983.
- [9] L. W. Weston et al, ``Neutron Capture Cross Sections in the keV Region Part II Spin-Orbit Coupling and the Optical Model,`` J, AP, 10, 477, 1960.

- [10] G.A. Linenberger and J.A.Miskel, ``Capture Cross Sections of Several Substances for Neutrons at Various Energies,`` R, LA-467, 1946.
- [11] W. Poenitz, ``Measurements of Activation Cross Sections,`` P, EANDC(E)- 66, 6, 1966.
- [12] V.G. Alpatov et al, ``Excitation of 107,109-Ag Isotopic States in the Fast Neutron Inelastic Scattering Reactions at the IBR-2 Reactor of JINR,`` J, YF, 60,(6), 970, 1997.
- [13] W. Augustyniak et al, ``Cross Sections for the Inelastic Scattering, (n,p) and (n,2n) Reactions on Ag-107 and Ag-109 Isotopes,`` J, NP/A, 247, 231, 1975.
- [14] I. Wagner and M.Uhl, ``Measurements of Some (n,p), (n,2n) and (n,ng) Cross Sections of Medium Heavy Nuclei,`` J, OSA, 108, 185, 1971.
- [15] T.B. Ryves et al, ``Silver Cross Sections for 14 MeV Neutrons,`` J, JP/G, 14, 77, 1988.
- [16] J.P. Gupta et al, ``Pre-equilibrium Emission Effect in (n,p) Reaction Cross Section at 14.8 MeV,`` J, PRM, 24, 637, 1985.
- [17] R. Prasad, D.C. Sarkar, ``Measured (n,p) Reaction Cross Sections and Their Predicted Values at 14.8 MeV,`` J, NC/A, 3, (3), 467, 1971.
- [18] V.N. Levkovskiy et al, ``Cross-sections of Reactions (n,p) and (n,a) at 14.8 MeV Neutron Energy,`` J, YF, 10, (1), 44, 1969.
- [19] B.P. Bayhurst and R.J. Prestwood, ``(n,p) and (n,a) Excitation Functions of Several Nuclei from 7.0 TO 19.8 MeV,`` J, JIN, 23, 173, 1961.
- [20] S.K. Mukherjee, ``Activation Cross Sections with 14 MeV Neutrons,`` J, PPS, 77, 508, 1961.
- [21] R.F. Coleman et al, ``Cross Sections for (n,p) and (n,a) Reactions with 14.5 MeV Neutrons,`` J, PPS, 73, 215, 1959.
- [22] B.G. Dzantijev et al, ``(n,a) Reactions of 14-MeV Neutrons with Cadmium,`` J, DOK, 113, (3), 537, 1956.

Table I : Parameters for optical model potential

Parameter (unit)	<sup>109</sup> Ag
V <sub>o</sub> (MeV)	48.25
V <sub>1</sub> (MeV)	0.2
r <sub>o</sub> (fm)	1.191
a <sub>v</sub> (fm)	0.503
W <sub>o</sub> (MeV)	6.901
r <sub>w0</sub> (fm)	1.32
a <sub>w</sub> (fm)	0.535
V <sub>so</sub> (MeV)	6.0
r <sub>so</sub> (fm)	1.249
a <sub>so</sub> (fm)	0.603
W <sub>1</sub> (MeV)	0.15
r <sub>w1</sub> (fm)	0.0
r <sub>1</sub> (fm)	0.0

Table II : Comparison of s-wave strength function

Nuclide	s-wave strength function	
	by OM*	by evaluation**
<sup>109</sup> Ag	0.66E-4	0.57E-4

\*By ABAREX at 1keV

\*\*Evaluation at resonance region[3]

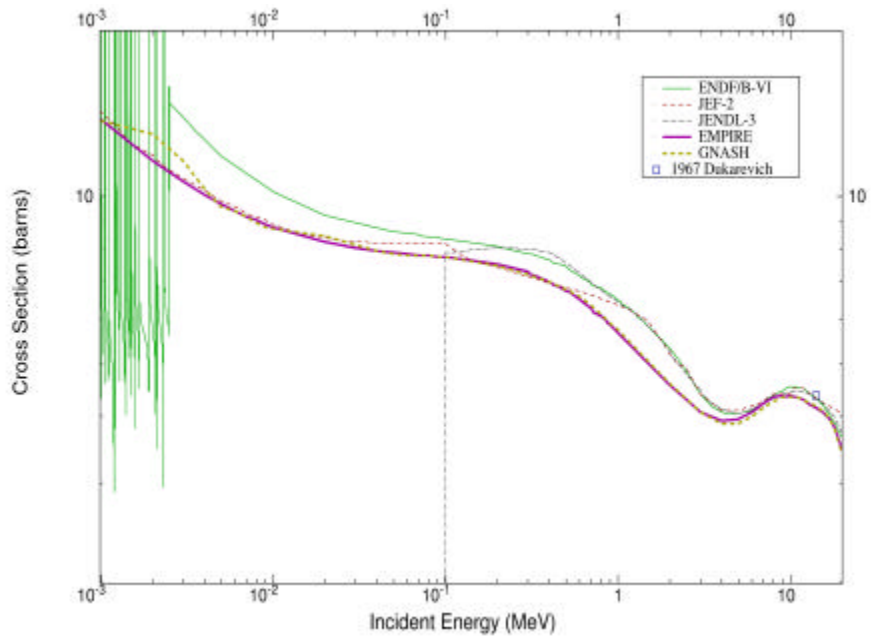


Fig. 1. Total cross section for  $^{109}\text{Ag}$ .

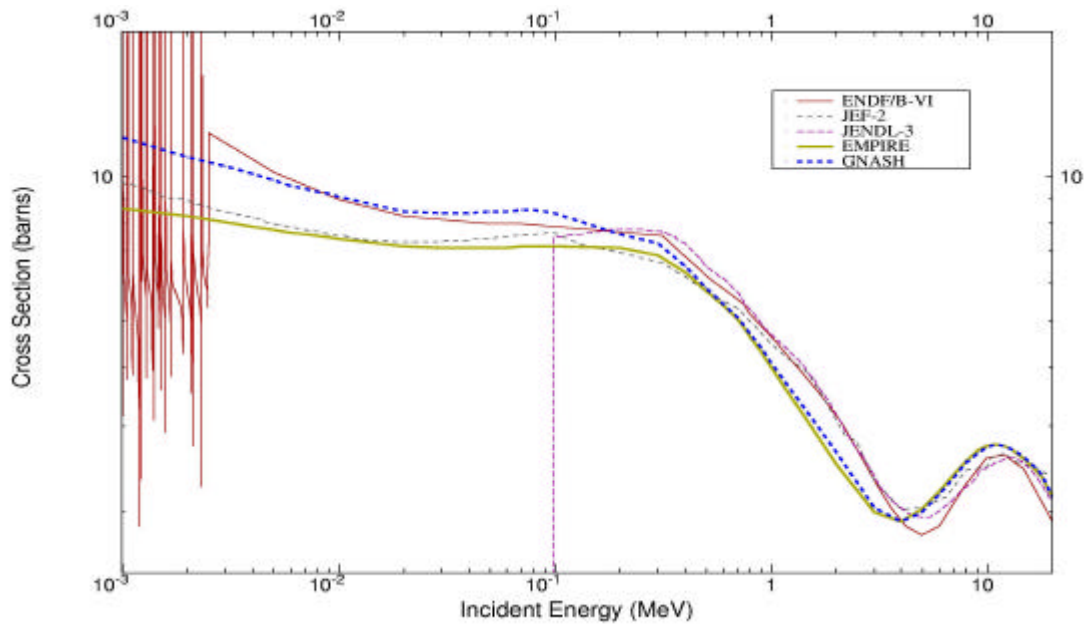


Fig. 2. Elastic scattering cross section for  $^{109}\text{Ag}$ .

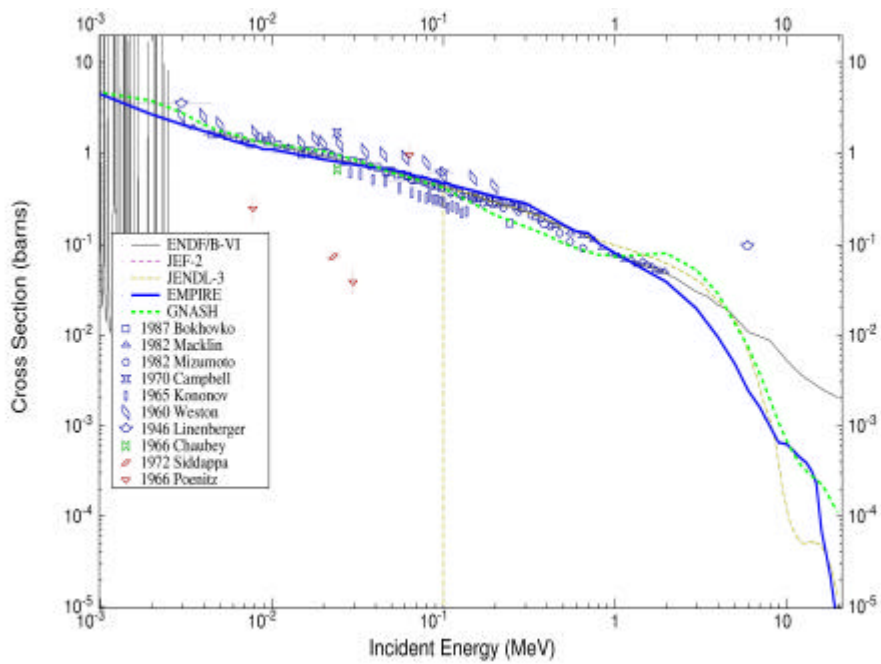


Fig. 3. Capture cross section for  $^{109}\text{Ag}$  in the whole energy range.

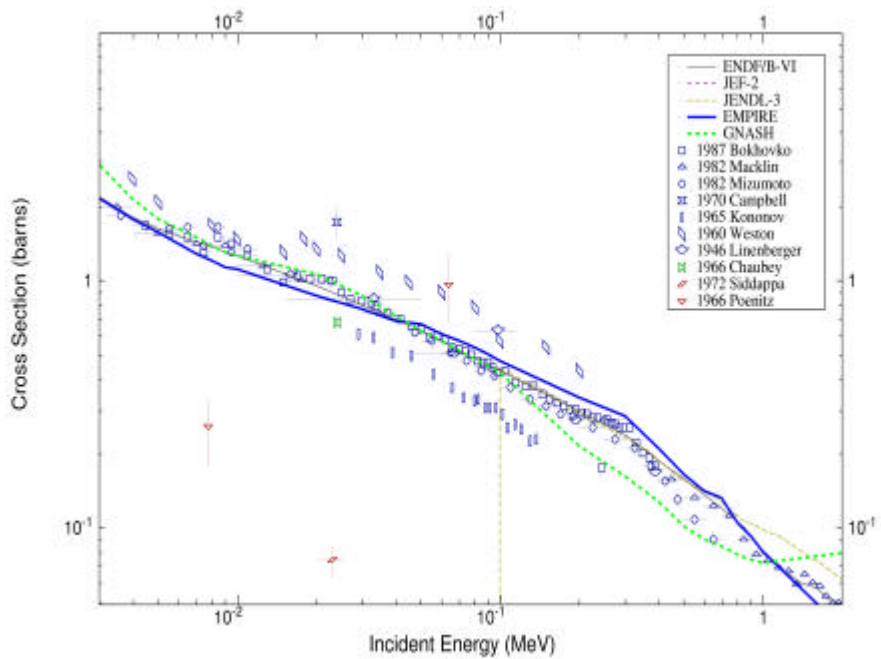


Fig. 4. Capture cross section for  $^{109}\text{Ag}$  in the measurement energy range.

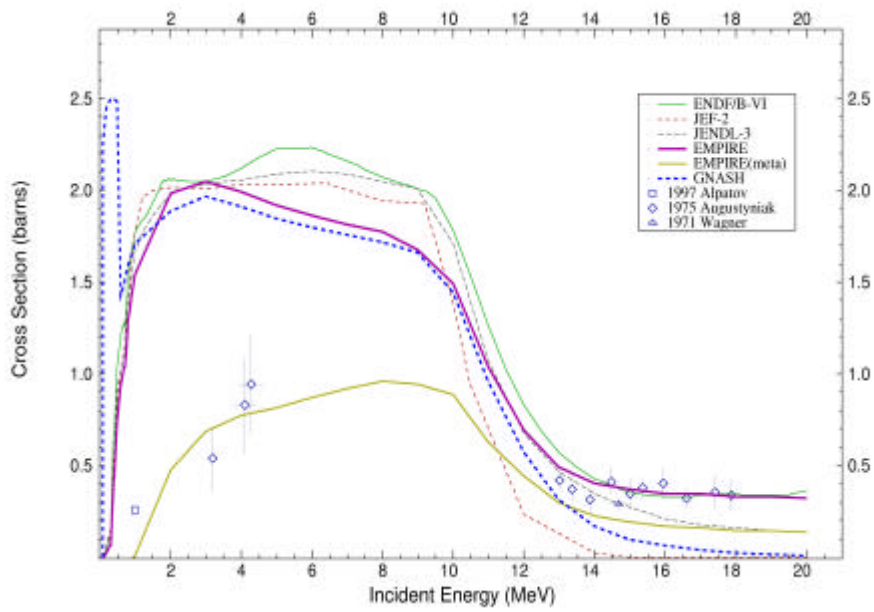


Fig. 5. Inelastic scattering cross section for  $^{109}\text{Ag}$ .

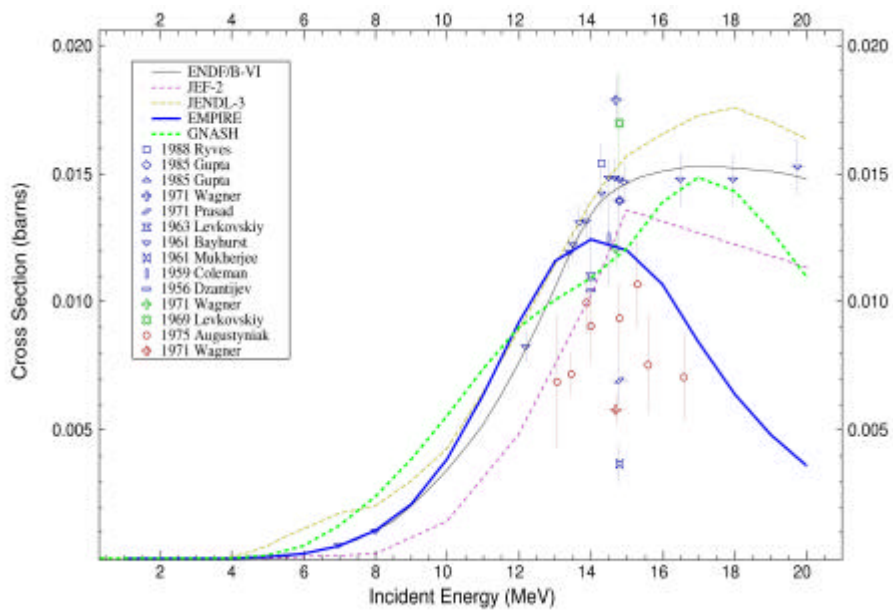


Fig. 6. (n, p) cross section for  $^{109}\text{Ag}$ .

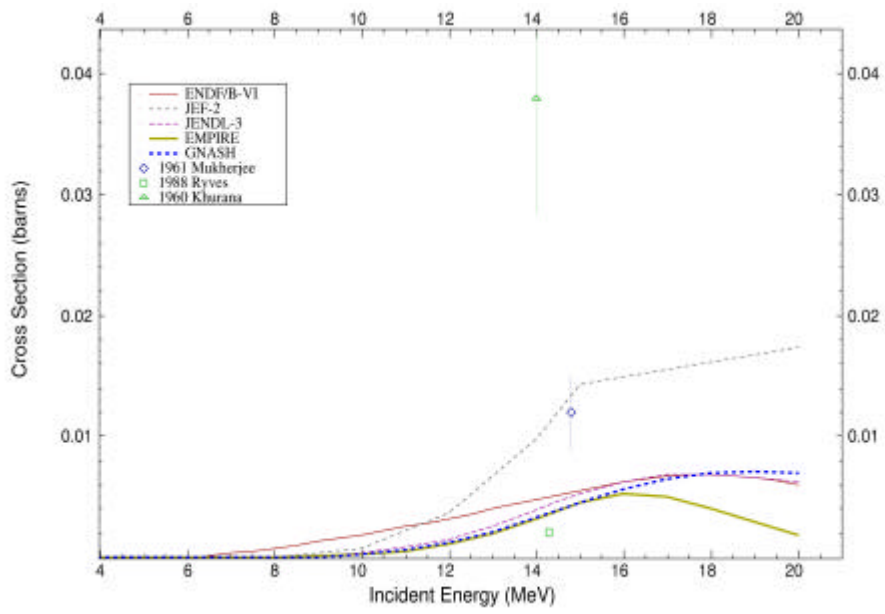


Fig. 7.  $(n, \alpha)$  cross section for  $^{109}\text{Ag}$ .

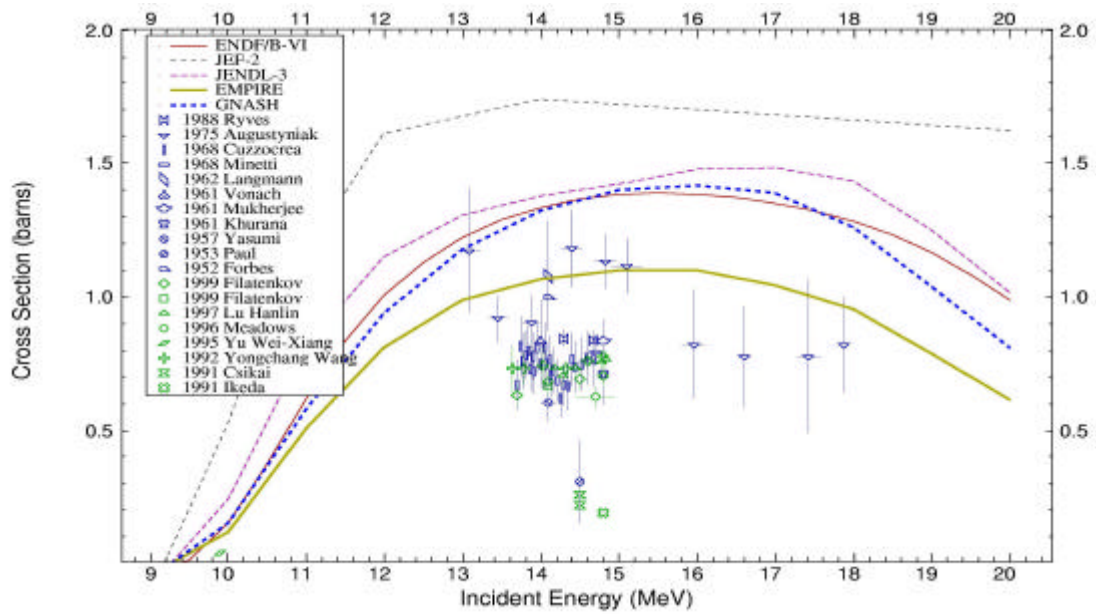


Fig. 8.  $(n, 2n)$  cross section for  $^{109}\text{Ag}$ .

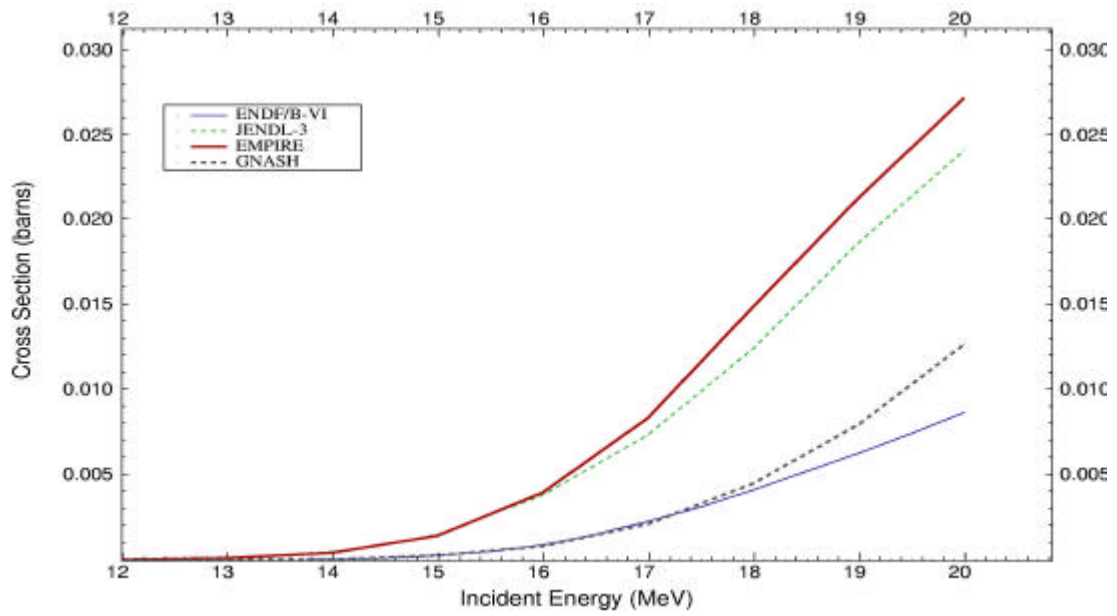


Fig. 9. (n, n $\alpha$ ) cross section for <sup>109</sup>Ag.

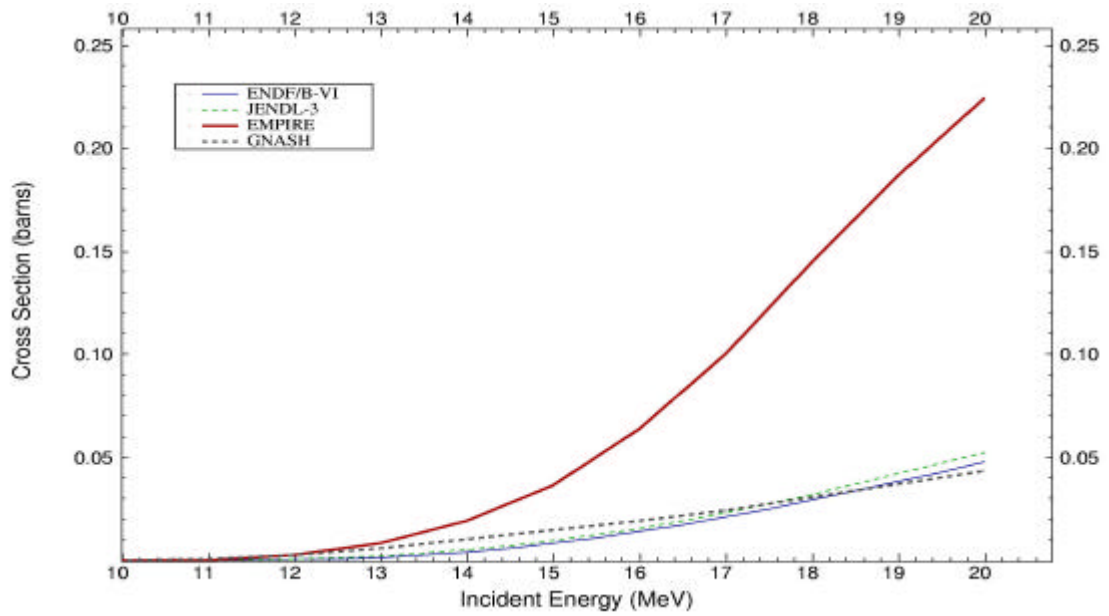


Fig. 10. (n, np) cross section for <sup>109</sup>Ag.